ChemComm

COMMUNICATION

View Article Online
View Journal | View Issue

Self-assembly of a tripeptide into a functional coating that resists fouling†

Sibaprasad Maity,‡ Sivan Nir,‡ Tal Zada and Meital Reches*

Cite this: *Chem. Commun.*, 2014, 50, 11154

Received 12th May 2014,
Accepted 22nd July 2014

DOI: 10.1039/c4cc03578j

www.rsc.org/chemcomm

This communication describes the self-assembly of a tripeptide into a functional coating that resists biofouling. Using this peptide-based coating we were able to prevent protein adsorption and interrupt biofilm formation. This coating can be applied on numerous substrates and therefore can serve in applications related to health care, marine and water treatment.

Biofouling is an undesirable process that results in the accumulation of organisms and their by-products on surfaces. The process initiates with the adsorption of bioorganic molecules onto a substrate, and proceeds with the attachment of organisms to this bioorganic layer.[1] In the case of bacteria, this process leads to the formation of a well-defined bacterial network, termed biofilm, which provides the bacteria with superior survival properties upon exposure to antibiotics.[2] Biofilm formation on medical devices and implants may lead to severe infections.[3] This phenomenon termed hospital-acquired infections is of major concern today for the health care system. In addition, biofouling has an enormous impact on the marine industry. This is due to the attachment of marine organisms such as barnacles and marine mussels to ships and other marine devices.[4] The thick heavy layer formed by these organisms causes delay in transportation and additional consumption of fuel.[5] In addition, the colonization of ship hulls has been linked to two major environmental pollutions, which are emission of gases into the atmosphere and incursion of invasive species into marine habitats.[6]

Antifouling materials alter the physical and/or chemical properties of the surface in order to prevent the accumulation of the organisms on the substrate.[1–4,7] The need for nontoxic antifouling materials led to the development of numerous approaches. These strategies include enzymatic degradation, sonication and chemical modification of the substrates.[1–4,7] Each approach has some disadvantages. These include low stability, short-term activity, limitation to specific surfaces and complicated and expensive synthesis or fabrication procedures.[8]

This communication presents a new rationally designed antifouling material formed by the self-assembly of a low-molecular weight peptide into a supramolecular coating. The peptide is a synthetic tripeptide that interferes with the first step of biofouling. We chose a peptide backbone for the design of this material since peptides are diverse, biocompatible, stable, and can spontaneously form ordered structures by self-assembly.[9] There are numerous reports in the literature on antibacterial peptides, however very few on peptides with antifouling activity. These include the ultra-low fouling natural peptides composed of negatively and positively charged residues in the form of either alternating or randomly mixed charge.[10] These peptides, however, are longer than the peptide proposed herein and require an alkanethiol for adhesion to gold.

The peptide sequence, which we designed, contains three elements that enable (i) its self-assembly into a coating, (ii) its adsorption onto any substrate and (iii) its antifouling activity (Fig. 1).

The element that we chose to direct the assembly of the peptide comprises two adjacent fluorinated phenylalanine residues. Due to aromatic interactions, the dipeptide diphenylalanine and its fluorinated analogues can self-assemble into highly ordered structures such as fibers and tubes.[9,11] We assumed that this motif will promote molecular recognition and direct the self-assembly of the peptide into a film. In addition, we expected that the carbon–fluorine bond of the fluorinated aromatic ring would lead to the formation of a "Teflon-like" material that will prevent the attachment of proteins to the surface and therefore will act as the antifouling motif. We chose to explore two variations of the peptide: one contains only one fluorine atom on each of the benzene rings (peptide **1**) and the other contains five (peptide **2**). The third amino acid of the peptide is 3,4-dihydroxy-L-phenylalanine (DOPA). This is the main constituent of mussel adhesive proteins (MAPs), the glue proteins of marine mussels.[12] These proteins can adhere to almost any substrate and survive harsh conditions such as tide and high salt concentration.[12] DOPA itself can adhere to various surfaces.[13]

Institute of Chemistry and The Center for Nanoscience and Nanotechnology, The Hebrew University of Jerusalem, Jerusalem 91904, Israel.
E-mail: meital.reches@mail.huji.ac.il

† Electronic supplementary information (ESI) available: Peptide synthesis, experimental details and additional figures. See DOI: 10.1039/c4cc03578j

‡ These authors contributed equally to this work.

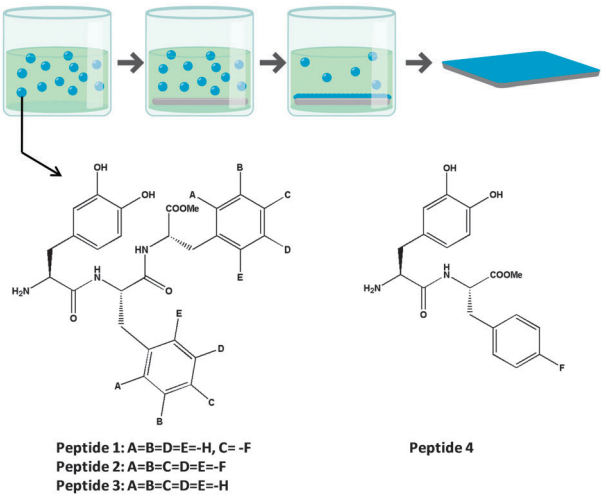

Fig. 1 The illustration in the upper panel shows the formation of a coating on a substrate by dip coating. The lower panel illustrates the molecular structures of the studied peptides.

We assumed that the insertion of the amino acid DOPA into the peptide sequence would as a glue and immobilizes the peptide on different substrates.

We compared the physical properties and antifouling activity of peptides **1** and **2** to two additional peptides: peptide **3**, which does not contain any fluorine atoms and a dipeptide (peptide **4**) that comprises the amino acid DOPA and one fluorinated phenylalanine residue (Fig. 1). To coat a substrate (*e.g.* gold, silicon, titanium, glass or stainless steel) with the peptide, we dipped bare substrates in the peptide solution. To determine if peptide **1** indeed generated a "Teflon-like" layer on the different substrates we measured their contact angle. As we assumed, the modified surfaces exhibited an increase in the contact angle, from 43° to 68°, indicating an increase in the substrate's hydrophobicity (Fig. 2c–j). Similarly, peptides **2–4** followed the same trend (Fig. S1, ESI†): peptide **2** which contains more fluorine atoms increased the contact angle of titanium to 83°. Due to its hydrophobic nature peptide **3** increased the contact angle of the substrate, however this increase was lower than the increase resulting from peptide **1**. The dipeptide, peptide **4**, increased the contact angle similarly to peptide **1** to 67°. We also found a correlation between the angle size and the concentration of the peptide solution, as the peptide concentration increased, the contact angle was larger (Fig. S2, ESI†). Due to the hydrophobic moieties of the peptides, water could not be used as a solvent system despite its high polarity. We used methanol as the solvent since it dissolved the peptide completely and at the same time allowed it to adhere the substrate. Since methanol is a toxic solvent, we also examined other solvents with different polarities. When we used solvents, such as acetone, ethanol and isopropanol, with polarities that resemble the polarity of methanol, the peptide-based coating self-assembled in a similar manner as it did in methanol (Fig. S3 and S4, ESI†). However, in solvents with high polarity, such as dimethylsulfoxide (DMSO) or 1,1,1,3,3,3-hexafluoro-2-propanol (HFP), the peptide dissolved but did not adhere to the substrate (Fig. S3, ESI†).

To characterize the topography of the modified surfaces we performed Atomic Force Microscopy (AFM) analysis of mica surfaces coated with the different peptides. AFM analysis clearly showed that the topography of the mica coated with peptide **1** was different from the topography of the bare mica. In addition, some spherical aggregates appeared on the coated substrate (Fig. 2). We detected similar topography for surfaces modified with peptides **2–4** (Fig. S5, ESI†). However, peptides **3** and **4** formed more aggregates on the surface than peptides **1** and **2**.

Using Attenuated Total Reflectance Fourier Transform Infrared (ATR-FTIR) spectroscopy, we studied if the peptides are indeed present on the substrate and what their configuration on the substrate is.[14] The bare titanium substrate has a typical peak at 880–870 cm^{-1} (Fig. 3a). This peak did not appear when the substrate was coated with peptide **1** and peptide **2** indicating the

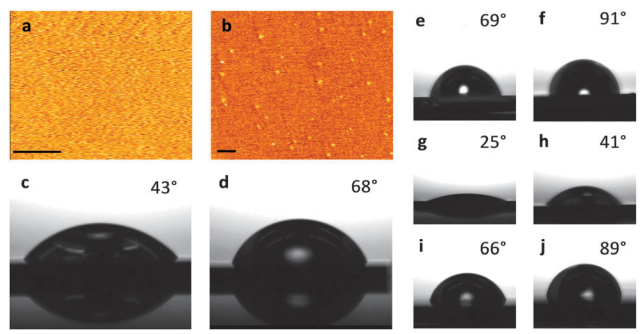

Fig. 2 Surface characterization of bare substrates *versus* substrates coated with peptide **1**. AFM topography images of (a) bare mica, (b) coated mica, the scale bars represent 500 nm. Contact angle measurements of (c) bare titanium, (d) coated titanium (e) bare gold (f) coated gold, (g) bare silicon, (h) coated silicon, (i) bare stainless steel, (j) coated stainless steel.

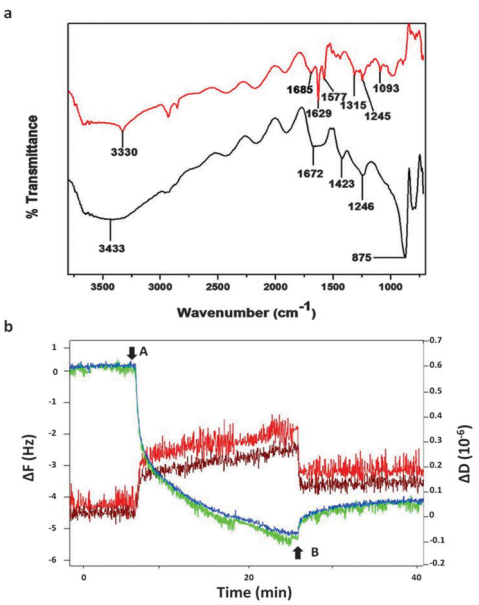

Fig. 3 (a) ATR-FTIR spectra of bare titanium (black) and titanium coated with peptide **1** (red). (b) Real-time QCM-D measurements of peptide **1**. Frequency overtones 5 and 7 are presented in green and blue respectively. Dissipation overtones 5 and 7 are presented in red and maroon respectively. Arrow A, indicates peptide addition, arrow B, washing with methanol.

formation of a coating on the substrate. Another informative IR frequency range is 3500–3200 cm^{-1} since a narrow peak at this frequency corresponds to the N–H stretching vibrations of the peptide. In addition, a broad peak in this range results from the vibration signal of the native oxide of the titanium.[15] In our experiments, a narrow peak appeared at 3330 cm^{-1} when the titanium surface was coated with peptide **1**. This IR peak suggests the binding of the peptide to the substrate (Fig. 3a). Similarly, a narrow N–H stretching band appeared between 3305 cm^{-1} and 3322 cm^{-1} for the surfaces modified with peptides **2–4** (Fig. S6, ESI†). In these cases the peaks were not as significant as in the spectrum of peptide **1**. Additional peaks in the region 1310–1000 cm^{-1} appeared in the spectra of all peptides. This region is characteristic of the C–F stretching band, however it overlaps with the region 1330–1200 cm^{-1} which is typical for amide III (Fig. S6, ESI†).[16] Therefore, the peaks in this region were also expected for peptide **3**.

The IR region 1800–1500 cm^{-1} is related to the stretching band of amide I and can indicate the secondary structure of the peptides. The ATR-FTIR spectrum of a substrate coated with peptide **1** comprises two peaks at 1685 cm^{-1} and 1629 cm^{-1} indicating an antiparallel beta-sheet.[17] For peptide **2** the amide I peak appeared at 1678 cm^{-1} and 1608 cm^{-1} indicating the same type of peptide secondary structures on the substrate (Fig. S6, ESI†).[17,18] The IR spectrum of peptide **4** had a peak at 1620 cm^{-1} which indicated a beta sheet structure. The higher peak, however, shifted to 1696 cm^{-1}, and another peak at 1655 cm^{-1} appeared. This peak may suggest alpha helical conformation for the supramolecular structure (Fig. S6, ESI†). Overall, this spectrum indicates that the coating formed by peptide **4** is less organized than the one formed by peptide **1**. An additional indication of the formation of a less homogenous and organized coating by peptide **4** is the low intensity of peaks, and a low signal to noise ratio of the spectrum when compared to the spectra of peptides **1** and **2**. Similarly, the peak related to the titanium substrate was also present in the ATR-IR spectrum of peptide **3**. The other regions of the spectrum had a low signal to noise ratio and significant peaks could not be detected. This is probably due to the tendency of this peptide to form spherical aggregates rather than a homogenous coating on the substrate. This prevented a complete contact with the ATR crystal, which is needed in order to obtain a good signal (Fig. S5, ESI†).

Using Quartz Crystal Microbalance with Dissipation monitoring (QCM-D) we studied the real-time adhesion of the peptides to titanium substrates. Each peptide was injected into a flow cell containing a titanium-coated sensor. The injection of peptide **1** resulted in changes both in frequency (ΔF) and dissipation (ΔD). This suggests that the peptide bonded to the sensor. Upon washing with methanol, we only observed small changes in frequency and dissipation; this indicates the formation of a stable film on the surface (Fig. 3b). Peptide **2** followed a similar trend, however, the frequency change was lower (Fig. S7, ESI†). This implies that the number of fluorine atoms had an effect on the adhesion of the peptide to the substrate. In the case of peptide **3**, the change in frequency was even lower. In addition, upon washing, the frequency changed again significantly, resulting in a total change of 0.5 Hz. This indicates that most of the peptide did not adsorb onto the sensor. Since QCM-D is a mass dependent technique, we expected a change in frequency that would be linearly dependent on mass. Because the mass ratio of peptide **1** and **4** is 0.7, we expected that the change in frequency for peptide **4** would be 3.5 Hz (Fig. 3b and Fig. S7, ESI†). However, the change in frequency was lower and equaled 1.5 Hz. In addition, the change in frequency for peptide **4** reached a plateau only after ~10 minutes, while peptides **1–3** did not attain a plateau in frequency even after 25 minutes (Fig. S7, ESI†). These QCM-D results along with the information obtained from the ATR-FTIR and AFM analysis further imply that the formation of a film by peptides **3** and **4** is less favorable under these conditions when compared with peptide **1**. The magnitudes of changes in dissipation are also very informative. The changes in dissipation observed for all peptides were around 0.1×10^{6}, characteristic of a rigid film.[19] This allowed us to use the Sauerbrey relation in order to calculate the mass adsorbed onto the sensor (Fig. S8, ESI†). The loaded mass/area was found to be 72.1 ± 0.4 ng cm^{-2}, 56 ± 2 ng cm^{-2}, 14 ± 3 ng cm^{-2} and 13 ± 2 ng cm^{-2} for peptides **1–4** respectively. These calculations can serve as a quantitative basis for our speculations regarding the poor coverage of peptides **2–4** in comparison to peptide **1**. It should be noted that the QCM-D experiments lasted 40 minutes and therefore measured only the beginning of the coating process.

Using X-ray Photoelectron Spectroscopy (XPS) analysis we characterized surfaces that underwent a prolonged incubation with the peptide to ensure the complete modification of the titanium substrates. When compared with a bare titanium, the signals resulting from the substrates coated with peptides **1–2** and **4** indicated the presence of fluorine (Fig. S9, ESI†). These signals indicated the deposition of the peptides on the surface. As expected, no fluorine signal was obtained from peptide **3**, however, the intensity of carbon and nitrogen signals was higher than the intensity of the signals obtained from bare titanium substrates. This indicated the deposition of peptide **3** on the surface (Fig. S9, ESI†). The average thickness of the peptide layer evaluated by the XPS analysis was 3.9 ± 0.1 nm, 4.2 ± 0.1 nm, 4.0 ± 0.1 nm, and 3.82 ± 0.04 nm for peptides **1–4** respectively. We also determined the thickness of the coating using ellipsometry. By fitting the measurement to the Cauchy film model,[20] which is suitable for organic coatings, we evaluated a thickness of 3.41 ± 0.05 nm, 5.2 ± 0.1, 4.61 ± 0.08 nm, and 3.66 ± 0.04 nm for peptides **1–4** respectively. These findings are in agreement with the results obtained by XPS analysis.

The formation of a biofouling community depends on the initial adsorption of bioorganic matter which mediates the subsequent attachment of organisms.[1] We, therefore, investigated the resistance of the peptide-based coating to protein adsorption. A bare and coated titanium substrate were incubated in a protein solution, either bovine serum albumin (BSA), or lysozyme (at a concentration of 150 μM for two hours at 37 °C). To determine the adsorbed amounts of the proteins on the substrates we used the non-interfering protein assay™ kit. The plot in Fig. 4a summarizes the adsorbed amounts of proteins onto bare and coated titanium substrates. Both BSA and lysozyme adsorbed onto the bare titanium substrate and in similar amounts onto the substrate coated with peptide **3** (Fig. 4a).

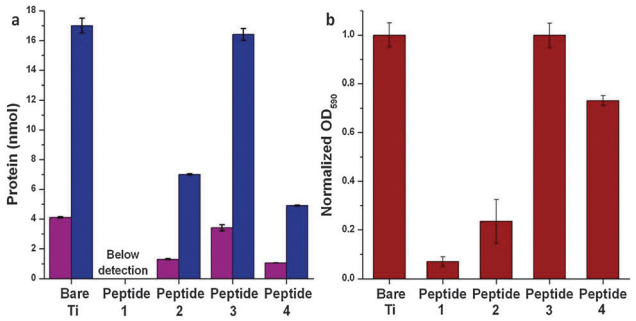

Fig. 4 Assessment of the antifouling activity of the studied peptides. Adsorbed amounts of (a) BSA (violet) and lysozyme (blue) to bare and coated titanium substrates with peptide **1–4**. (b) Optical density quantification of the accumulated *P. aeruginosa*, on bare and coated titanium substrates with peptides **1–4**. Error bars represent standard deviations (n = 9).

Both proteins also adsorbed onto substrates coated with peptide **2** or **4**. The amounts of proteins adsorbed onto these substrates were smaller than those that adsorbed onto the bare substrate. However, the amount of proteins, either BSA or lysozyme, adsorbed onto a titanium substrate coated with peptide **1** was negligible and below the detection limit of the kit (Fig. 4a). Overall these results demonstrate that in order to achieve antifouling activity the peptide must contain fluorinated phenylalanine residues. In addition, the best configuration is of peptide **1**.

To assess the bacterial attachment to the surface, bare and peptide-coated substrates were incubated in inoculums of *Pseudomonas aeruginosa* and *Escherichia coli* for 9 and 96 hours respectively. These incubation times allowed the formation of a biofilm by the different pathogenic bacterial strains. After incubation we stained the substrates with 2%(w/w) Crystal Violet (CV).[21] Using an optical microscope we observed a thick and dense purple layer on the bare titanium surface which indicated a thick bacterial coverage of the substrate, while on the coated titanium we only detected sparse bacteria (Fig. S9, ESI†). To quantify these results, we extracted the CV dye from the bacteria and measured its absorbance.[22] The absorbance of the CV is proportional to the number of bacteria attached to the surface. The plot in Fig. 4b shows that the best antifouling activity is achieved by peptide **1**. For surfaces coated with peptide **1** and incubated with *P. aeruginosa* we observed a reduction of 93% in the amount of CV on a coated substrate when compared to a bare substrate (Fig. 4b). For surfaces coated with peptide **1** and incubated with *E. coli*, a reduction of 74% in the amount of CV was detected (Fig. S10, ESI†). As our results on the nature of the coating indicate that the best coating is formed by this specific peptide when compared to peptides **2–4**, we indeed expect that its antifouling activity would be the most efficient.

In summary, we suggest a new antifouling material based on the self-assembly of a tripeptide. The peptide design includes the amino acid DOPA as the adsorption motif, the diphenylalanine as the element that directs the self-assembly process and fluorine atoms as the antifouling agents. The application of the peptide on the surface is very simple as it occurs spontaneously. We demonstrated the formation of a coating on various substrates and presented its ability to disrupt the process of biofouling. The peptide presented here can be useful in a large variety of applications. Its coating on medical devices or hospital equipment can lead to a reduction in the number of hospital-acquired infections. In addition, it may also be useful in preventing the adsorption of aqueous and marine organisms and assist when dealing with water treatment and marine fouling.

This work was supported by the Israeli Ministry of Industry, Trade and Labor. S.M acknowledges the support of the Israel Council for Higher Education. S.N acknowledges the support of the Hebrew University Center for Nanoscience and Nanotechnology. We thank Ms A. Zoabi and Dr R. Abu-Reziq for their help with HPLC analysis and the help of Dr V. Gutkin with XPS analysis.

Notes and references

1 C. M. Kirschner and A. B. Brennan, *Annu. Rev. Mater. Res.*, 2012, **42**, 211.
2 H. C. Flemming, *Appl. Microbiol. Biotechnol.*, 2002, **59**, 629.
3 R. L. Meyer, A. Arpanaei, S. Pillai, N. Bernbom, J. J. Enghild, Y. Y. Ng, L. Gram, F. Besenbacher and P. Kingshott, *Colloids Surf., B*, 2013, **102**, 504.
4 M. E. Callow and J. A. Callow, *Biologist*, 2002, **49**, 10.
5 M. P. Schultz, *Biofouling*, 2007, **23**, 331; K. Drescher, Y. Shen, B. L. Bassler and H. A. Stone, *Proc. Natl. Acad. Sci. U. S. A.*, 2013, **110**, 4345.
6 J.-P. Marechal and C. Hellio, *Int. J. Mol. Sci.*, 2009, **10**, 4623; E. S. Poloczanska and A. J. Butler, *Biofouling*, Wiley-Blackwell, 2010, p. 333.
7 I. Banerjee, R. C. Pangule and R. S. Kane, *Adv. Mater.*, 2011, **23**, 690; P. Harder, M. Grunze, R. Dahint, G. M. Whitesides and P. E. Laibinis, *J. Phys. Chem. B*, 1998, **102**, 426; X. Khoo, P. Hamilton, G. A. O'Toole, B. D. Snyder, D. J. Kenan and M. W. Grinstaff, *J. Am. Chem. Soc.*, 2009, **131**, 10992; R. G. Nuzzo, *Nat. Mater.*, 2003, **2**, 207; A. K. Epstein, T.-S. Wong, R. A. Belisle, E. M. Boggs and J. Aizenberg, *Proc. Natl. Acad. Sci. U. S. A.*, 2012, **109**, 13182; J. A. Callow and M. E. Callow, *Nat. Commun.*, 2011, **2**, 244; S. Krishnan, C. J. Weinman and C. K. Ober, *J. Mater. Chem.*, 2008, **18**, 3405; D. L. Schmidt, R. F. Brady, K. Lam, D. C. Schmidt and M. K. Chaudhury, *Langmuir*, 2004, **20**, 2830.
8 S. Han, C. Kim and D. Kwon, *Polymer*, 1997, **38**, 317; E. Lindner, *Biofouling*, 1992, **6**, 193.
9 J. D. Hartgerink, E. Beniash and S. I. Stupp, *Science*, 2001, **294**, 1684; D. T. Bong, T. D. Clark, J. R. Granja and M. R. Ghadiri, *Angew. Chem., Int. Ed.*, 2001, **40**, 988; X. Y. Gao and H. Matsui, *Adv. Mater.*, 2005, **17**, 2037; V. Jayawarna, M. Ali, T. A. Jowitt, A. E. Miller, A. Saiani, J. E. Gough and R. V. Ulijn, *Adv. Mater.*, 2006, **18**, 611; M. Venanzi, G. Pace, A. Palleschi, L. Stella, P. Castrucci, M. Scarselli, M. De Crescenzi, F. Formaggio, C. Toniolo and G. Marletta, *Surf. Sci.*, 2006, **600**, 409; S. Maity, P. Jana, S. K. Maity and D. Haldar, *Langmuir*, 2011, **27**, 3835; A. N. Rissanou, E. Georgilis, E. Kasotaids, A. Mitraki and V. Harmandaris, *J. Phys. Chem. B*, 2013, **117**, 3962.
10 S. Chen, Z. Cao and S. Jiang, *Biomaterials*, 2009, **30**, 5892–5896.
11 M. Reches and E. Gazit, *Phys. Biol.*, 2006, **3**, S10; S. Yuran, Y. Razvag and M. Reches, *ACS Nano*, 2012, **6**, 9559; S. Maity, S. Nir and M. Reches, *J. Mater. Chem. B*, 2014, **2**, 2583.
12 J. H. Waite and M. L. Tanzer, *Science*, 1981, **212**, 1038.
13 H. Lee, S. M. Dellatore, W. M. Miller and P. B. Messersmith, *Science*, 2007, **318**, 426; H. Lee, N. F. Scherer and P. B. Messersmith, *Proc. Natl. Acad. Sci. U. S. A.*, 2006, **103**, 12999.
14 K. B. Alici and I. F. Gallardo, *Sci. Rep.*, 2013, **3**, 1.
15 A. M. Bobrova, I. G. Zhigun, M. I. Bragina and A. A. Fotiev, *J. Appl. Spectrosc.*, 1968, **8**, 59.
16 N. Baskali, F. Gaillard, P. Lanteri and V. Roucoules, *Anal. Chim. Acta*, 2004, **512**, 231.
17 P. I. Haris and D. Chapman, *Biopolymers*, 1995, **37**, 251.
18 E. Cerf, R. Sarroukh, S. Tamamizu-Kato, L. Breydo, S. Derclaye, Y. F. Dufrene, V. Narayanaswami, E. Goormaghtigh, J.-M. Ruysschaert and V. Raussens, *Biochem. J.*, 2009, **421**, 415.
19 R. Bordes, J. Tropsch and K. Holmberg, *Langmuir*, 2010, **26**, 3077.
20 *Handbook of ellipsometry*, ed. H. Tompkins and E. A. Irene, Springer, 2005.
21 T. J. Beveridge, *Biotech. Histochem.*, 2001, **76**, 111.
22 S. Stepanovic, D. Vukovic, I. Dakic, B. Savic and M. Svabic-Vlahovic, *J. Microbiol. Methods*, 2000, **40**, 175.